Key Engineering Materials
ISSN: 1662-9795, Vol. 919, pp 35-46
doi:10.4028/p-4k539k

Submitted: 2021-08-19
Accepted: 2021-10-12
Online: 2022-05-11

Analytical Approach for Modelling the Pull-Out Mechanism of Recycled Synthetic Fibres in Fibre-Reinforced Concrete (FRC)

Andrea Sorzia[1,a], Cesare Signorini[2,b*], Valentina Volpini[3,c], and Pietro Di Maida[1,3,d]

[1]Department of Sciences and Methods for Engineering, University of Modena and Reggio Emilia. Via G. Amendola 2, 42122 Reggio Emilia, Italy

[2]Interdepartmental Research Centre "CRICT", University of Modena and Reggio Emilia. Via P. Vivarelli 10, 41125 Modena, Italy

[3]Interdepartmental Research Centre "En&Tech", University of Modena and Reggio Emilia. Via G. Amendola 2, 42122 Reggio Emilia, Italy

[a]andrea.sorzia@unimore.it, [b]cesare.signorini@unimore.it, [c]valentina.volpini@unimore.it, [d]pietro.dimaida@unimore.it

Keywords: Pull-Out Test, Creep, Fibre-Reinforced Concrete (FRC), Frictional-Hardening Interface Behaviour, Constitutive Law

Abstract. This study presents a simple one-dimensional analytical model describing the pull-out process of an elastic fibre embedded in a cement matrix, which captures the ductile behaviour of Fibre Reinforced Concrete (FRC) elements. The shear stress arising at the frictional interface between fibre and matrix during the pull-out is assumed to increase with the slippage distance, as a consequence of the growing abrasion of the fibre surface. The equilibrium conditions between the external axial load and the interfacial shear stress are imposed with reference to the undeformed configuration. The model is validated through comparison with both experimental data obtained by testing partially recycled polymeric fibres embedded in a cement matrix, and several datasets available in the literature comprising polypropylene fibres with and without silica coatings. The proposed model can properly describe the response of synthetic fibres that exhibit considerable axial elongation and slip-hardening interface behaviour. However, it may also predict the non-linear relation between the tensile load and the fibre displacement for different kinds of fibre, by setting adequately the constitutive parameters.

Introduction

Concrete has been largely adopted in construction industry owing to its numerous advantages, like good compressive performance, practicality of manufacturing, and low cost. Nowadays, concrete represents the most widespread construction material worldwide. The synergy between concrete and steel has been traditionally established to overcome the main typical shortcomings of concrete and cementitious conglomerates in general, namely pronounced brittleness, poor tensile and impact resistance [1, 2, 3]. More recently, the adoption of fibres in concrete has gained increasing popularity in the scientific community, to confer further bearing capacity and dissipation resources to concrete [4]. In this direction, the use of either textiles or dispersed fibres represents a good option, especially to achieve a significant increase in the ductility in the occurrence of dynamic and/or repeated loadings [5], alongside a remarkable enhancement of the overall performance of the composite system after attaining the peak load. This particular kind of materials are usually regarded as strain-hardening cement-based composites (SHCC) [6, 7]. Generally speaking, dispersed fibres have been included in cement-based materials in order to limit or even eliminate the use of rebar, and this composites are generally regarded as fibre-reinforced concrete (FRC). In more recent times, the scenario of reinforcing fibres has enlarged significantly, moving through different materials (e.g. glass, steel, plastic, carbon) and geometries (e.g. micro and macro, hooked or straight). The random distribution of fibres within the matrix provides the composite with a uniform reinforcement with undeniable beneficial effects, also by reducing or even hindering cracks formation, eventually improving the long-term performance and

the fracture toughness [8]. For this reason, fibres in concrete may be considered as an important provision against brittle failure modes [9, 10] and undesired anti-dry-shrinkage cracking [11]. Focusing on the material constituting the fibres, polymers have turned out to represent a promising solution, for their attractive advantages over steel. Indeed, polymeric macro-fibres have been produced and commercialised for structural purposes owing to their lightness, chemical inertness, attitude to recycling [12, 13], easier storage and handling, and fire resistance, through their marked "anti-spalling" attitude [14]. Nonetheless, the chemical inertness of most polymeric macromolecules (especially polyolefins), which induces huge benefits in terms of durability, also represents the main weakness, since it prevents the fibres to adhere with cementitious matrices [15]. For this reason, manufacturers have developed new fibre shapes (e.g. crimping and embossing) and surface chemical treatments [16, 17] to increase the bond strength to the surrounding concrete matrix, working on both the mechanical and the chemical gripping. In this direction, several techniques have been proposed, like, e.g., chemical etching, functional coatings, plasma and ozone treatments [18, 19]. However, a definitive solution has not been established so far, and the adhesion is still an open research debate. Recently, a couple of studies carried out by Di Maida et al. [15] and Signorini et al. [17] has pointed out the opportunity to increase the bond strength of macro-synthetic (namely polypropylene, PP) fibres through a chemical nano-treatment consisting in the implantation of silica nano-particles on the surface of the fibres. Both the proposed treatments are obtained with a sol-gel process and induce a higher density of the interface transition zone (ITZ), thus improving the bonding properties. Pull-out tests on PP fibres embedded in a cementitious mortar were conducted and the maximum load and energy necessary for the complete extraction of a single fibre were measured. Experimental evidence shows that the magnitude of load-displacement curve notably increases for treated fibres, in particular after the complete debonding, namely at the pull-out phase. This pull-out phase, when the highest bond strength is involved, is very important in FRC post-cracking mechanism since it allows a large energy absorption and dissipation before the collapse of structural elements [20].

The present work shows the results of an experimental characterisation of the pull-out behaviour of partially recycled plastic fibres embedded in a cement-based matrix. A simple one-dimensional analytical model for the pull-out process is also proposed, further simplifying the formulation discussed by Sorzia et al. [21] and Radi et al. [22]. The model involves two different stages, namely debonding and pull-out, and is applied to describe the behaviour of the aforementioned partially recycled plastic fibres. The pull-out performance and constitutive law parameters obtained for recycled fibres are eventually compared to the ones retrieved for virgin PP fibres, exploiting the experimental findings by Di Maida et al. [15] and Signorini et al. [17], including the case of silica-coated PP fibres. In the present dissertation, the viscous contribution to the overall strain of the fibres is taken into account through the Maxwell model and then duly neglected. The validity of the model can be extended to various types of fibres having different constitutive interfacial laws (like, e.g., steel). Finally, a critical comparison with the model by Radi et al. [22] is considered in order to appreciate the differences between the two approaches.

Experimental Investigation

Raw materials

Partially recycled synthetic cylindrical draw-wire fibres are supplied by PlasticFibre Srl (Anzola Emilia, Italy), and consist of a blend of virgin polypropylene (PP) (30%) and a recycled portion (70%), made of polyethylene terephthalate (PET) and polyethylene (PE) in variable proportions. The recycled portion of the blend is retrieved from low-grade waste obtained by the industrial processing of food packaging, and the mechanical properties in bending of fibre-reinforced cementitious conglomerates are described in the paper by Signorini and Volpini [13]. The mortar consists of a commercially available cement-based conglomerate for structural restoration of concrete covers, whose mechanical properties are reported by Signorini et al. [17].

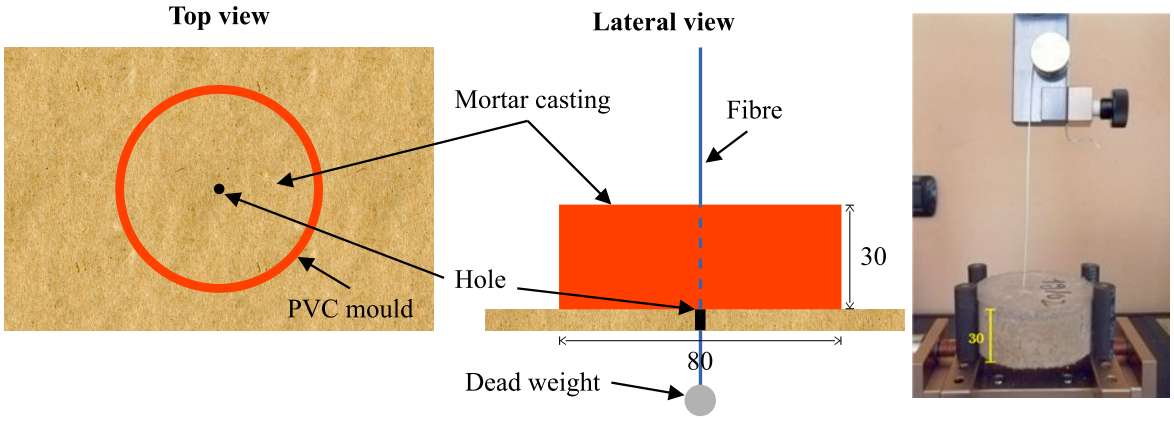

Fig. 1: *

Fig. 2: *

(a)

(b)

Fig. 3: Set-up for specimens manufacturing (a) and test set-up for pull-out tests (b). [Dimension are in mm]

Specimen manufacturing and pull-out test procedure

Pull-out tests are carried out on synthetic fibres in order to evaluate the peak stress and the dissipated energy due to friction. Specimens are manufactured using special polyvinyl-chloride (PVC) cylindrical moulds possessing a diameter of 80 mm, for casting the mortar block. PVC cylinders having thickness of 30 mm, are applied on a wooden support, properly drilled in the centre of each mould. This ensures the vertical alignment of the fibre during the mortar casting, see Fig.3a. Then, fibres are placed vertically in the correspondence of the central axis of the cylindrical tube and left passing through the hole in the middle. At the lower end of the fibre, a dead weight is applied to ensure verticality, whereas at the top, the fibre is firmly attached to a steel rod. Before casting in place the mortar within the PVC mould, a silicon-based lubricant is applied on the internal part of the tube and on the base support. Mortar blocks are stripped after 7 days and then left completing the hardening process for further 21 days at ambient conditions [17]. Fig.3b schematically shows the test set-up. Tests are carried out on an Universal Testing Machine (UTM) equipped with a 1 kN load cell. In the fixed cross-head of the machine the 30-mm-thick mortar cylinder is restraint by a tight clamping system. Connected to the upper movable cross-head of the UTM, the draw-wired fibre is wound up on a bobbin and the end is properly clamped. Tests are conducted at a fixed displacement rate equal to 1 $\mathrm{mm\,min^{-1}}$, in accordance with the protocol established by Signorini et al. [17].

Analytical Model

In this section, we present a simple one-dimensional analytical model, which properly describes the pull-out test of a synthetic fibre embedded in a cement-based matrix and loaded by an external tensile force aligned with the fibre axis. The frictional mechanism between the fibres and the cementitious matrix is described by a hardening non-linear shear stress law involving three parameters. The model neglects the cement matrix deformation and the Poisson effect of the fibre [23, 24]. Furthermore, it considers arbitrary large displacements of the fibre, but infinitesimal deformations, namely the equilibrium conditions on the undeformed configuration, substantially simplifying the approach. The deformation aliquot due to viscosity is taken into account through the Maxwell viscoelastic scheme and then discarded. Indeed, the viscous contribution during testing is likely significant for synthetic fibres, generally prone to long-term elongations. Two main phases are then postulated:

- First, a *debonding phase*, during which fibre detaches from the matrix starting from the outer section to the inner ones. In this phase, a pseudo-linear elastic relationship is established between the applied load and the longitudinal displacement of the end cross section of the fibre.

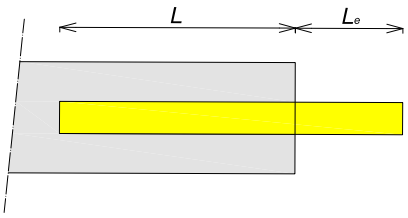

Fig. 4: *

(a)

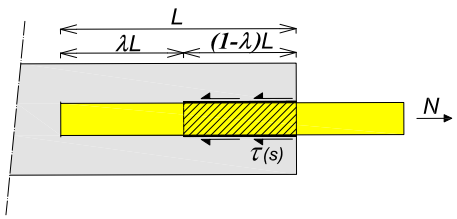

Fig. 5: *

(b)

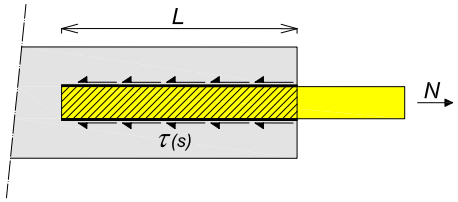

Fig. 6: *

(c)

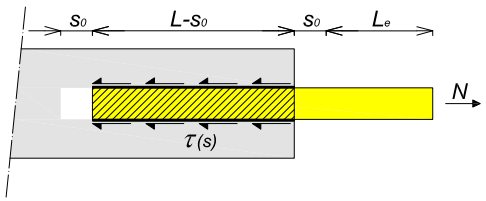

Fig. 7: *

(d)

Fig. 8: Constituent stages of pull-out mechanism in FRC: (a) initial stage, (b) debonding stage, (c) debonding-pull-out transition, and (d) pull-out stage

- After the complete detachment occurs, the *pull-out phase* is triggered, up to the complete extraction of the fibre from the matrix.

In both debonding and pull-out phases, the shear stress developing between the fibres and the surrounding matrix is described by a phenomenological law involving three constitutive parameters. The analytical results are compared with the experimental data obtained in the present study out of pull-out tests on recycled fibres in a cement-based mortar and extended to other relevant investigations [15, 17].

Governing equations

We consider a fibre embedded in a cement matrix for a length L and subjected to a tensile load N, as depicted in the schematic of Fig.8(a). The abscissa x denotes the position of the fibre section in the undeformed configuration. Since the matrix is assumed to be a rigid bulk material, $s(x)$ represents the differential slip of the fibre cross section with respect to the embedding medium at the abscissa x. Once the external load N is applied at the outer section of the fibre, the fibre starts slipping according to the two distinct phases previously illustrated, namely debonding and pull-ot stages, shown in Figure 8(b) and (d), respectively. During the debonding stage, the rate of the fibre surface involved in the debonding process increases progressively as the axial force arises, ensuring the fulfilment of the balance conditions between the load N and the shear force exerted at the interface of the debonded portion of the fibre. Therefore, the detachment from the outer section of the fibre $(1-\lambda)L$ varies from 0 to L at the end of the debonding stage, as in Figure 8(c). Indeed, the transition step between the full debonding and the beginning of the actual pull-out phase occurs as soon as the whole fibre surface is detached from the matrix. In the pull-out stage, the displacement of the inner section of the fibre s_0 varies from 0 to L at the end of the test, namely when the fibre is completely extracted from the matrix. While the fibre slips, the interface friction stress grows, due to the increase in the fibre abrasion and the release of concrete debris surrounding the cementitious matrix. Also, the possible presence of surface treatments is responsible for a progressive effectiveness increase of the interphase interaction [19]. The relationship between the shear stress τ arising around the surface of the fibre vs the slippage distance of the fibre s has been chosen properly, in order to account for such a phenomenon in a simple

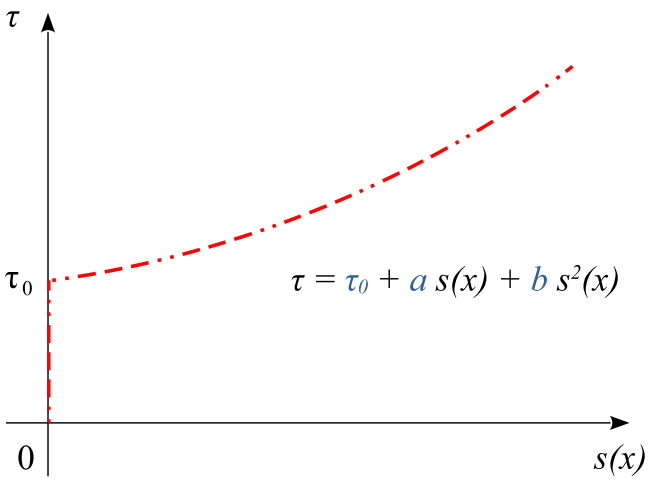

Fig. 9: Interface constitutive law between the interfacial shear stress τ and slippage distance s.

way [21], as

$$\tau(s) = \tau_0 + as + bs^2, \tag{1}$$

depicted in Fig. 9. In the Eq.(1), the constant parameters a, b and c should be calibrated to describe the fibre-to-matrix interaction.

Debonding and pull-out phase

By supposing that no axial loads act on the initial section of the fibre at $x = 0$, the axial load $N(x)$ acting on the extreme section of the fibre at abscissa x reads

$$N(x) = \pi d \int_0^x [\tau_0 + as(t) + bs^2(t)]dt, \qquad \begin{array}{ll} 0 \le x \le L - \lambda L & \text{in debonding stage} \\ 0 \le x \le L - s_0 & \text{in pull-out stage} \end{array} \tag{2}$$

where the adimensional parameter $\lambda \in [0,1]$ as depicted in Fig. 8. The axial strain of the fibre at the same abscissa x turns out to be

$$\varepsilon(x) = \frac{N(x)}{EA} = \frac{ds}{dx}. \tag{3}$$

By deriving $\varepsilon(x)$ from Eq.(3) with respect to x, where the cross section of the fibre is $A = \frac{\pi d^2}{4}$, one obtains

$$\frac{d^2s}{dx^2}(x) = \frac{4}{Ed}\left[\tau_0 + as(x) + bs^2(x)\right], \tag{4}$$

or, in a more compact form,

$$\frac{d^2s}{dx^2}(x) - Bs^2(x) - As(x) = C, \tag{5}$$

with $A = \frac{4a}{Ed}$, $B = \frac{4b}{Ed}$, $C = \frac{4\tau_0}{Ed}$.

In order to solve the ODE (5), we consider $p(s) = s'(x)$, thus Eq.(5) can be written as

$$p\frac{dp}{ds} - Bs^2(x) - As(x) = C, \tag{6}$$

being

$$\frac{d^2s}{dx^2}(x) = \frac{dp}{ds}s, \qquad p\frac{dp}{ds} = \frac{1}{2}\left(\frac{dp}{ds}\right)^2. \tag{7}$$

Then, integrating Eq.(6) with respect to s and then with respect to x one obtains

$$p(s) = \sqrt{2Cs + \frac{2}{3}Bs^3 + As^2 + 2C_0} = \varepsilon(x) \tag{8}$$

where C_0 is a constant of integration and

$$\int_{x_0}^{x} dx = \int_{s(x_0)}^{s(x)} \frac{ds}{\sqrt{2Cs + \frac{2}{3}Bs^3 + As^2 + 2C_0}}. \tag{9}$$

The proper boundary conditions (BCs) must be imposed in each phase, in order to define C_0. In the debonding phase, the BCs at $x = 0$ are $s(0) = 0$ and $\varepsilon(0) = 0$, thus Eq.(8) gives $C_0 = 0$, whereas Eq.(9), for $x_0 = 0$ and $x = L - \lambda L$, gives

$$\lambda = 1 - \frac{1}{L}\int_{0}^{s(L-\lambda L)} \frac{ds}{\sqrt{2Cs + \frac{2}{3}Bs^3 + As^2}}. \tag{10}$$

The parameter λ ranges from 0 to 1 during the debonding phase and the axial displacement of the outer section of the fibre $s_2 = s(L - \lambda L)$ is evaluated from Eq.(10), whereas its axial strain $\varepsilon_2 = \varepsilon(L - \lambda L)$ is assessed from Eq.(8).

In the pull-out phase, the BCs at $x = 0$ require $s(0) = s_0$ and $\varepsilon(0) = 0$, thus Eq.(8) gives $C_0 = -(Cs_0 + \frac{B}{3}s_0^3 + \frac{A}{2}s_0^2)$, meanwhile Eq.(9), for $x_0 = 0$ and $x = L - s0$, reads

$$s_0 = L - \int_{0}^{s(L-s_0)} \frac{ds}{\sqrt{2Cs + \frac{2}{3}Bs^3 + As^2 + C_0}}. \tag{11}$$

Then, the axial displacement $s_2 = s(L - s_0)$ is calculated from Eq.(11), whereas $\varepsilon_2 = \varepsilon(L - s_0)$ follows from Eq.(8).

The three parameters of the constitutive model τ_0, a, b, according to Eq.(1), are determined by fitting the curve obtained from Eq.(8), (10) and (11), during debonding and pull-out phases, with the averaged curve of several experimental tests, included the one presented in this paper, dealing with recycled cylindrical plastic fibres [15, 17]. Since the analytical model accounts for the elastic contribution of the displacement s_2 in debonding and pull-out phases but it does not account for the elastic contribution of the rigid motion s_0 outer to the matrix during the pull-out, this contribution is added apart. Similarly, the experimental data recorded during the test account for the elastic contribution of the outer portion of the fibre $L_e = 110\,\text{mm}$ placed between the cement matrix and the actuator, that was computed apart too.

Viscous contribution

To properly take into account the viscous deformation undertaken by the fibres during testing, a key passage of the model consists in splitting the elastic and the delayed strains due to viscosity. Indeed, owing to the considerable time required to accomplish the pull-out tests (more than 30 minutes) the fibre exhibits a significant elongation that it is not recovered completely at the end of the pull-out test, as a consequence of the pronounced viscous behaviour of plastics, like, among the others, PP, PE and PET. This additional strain leads to an inaccurate calibration of the constitutive parameters of the

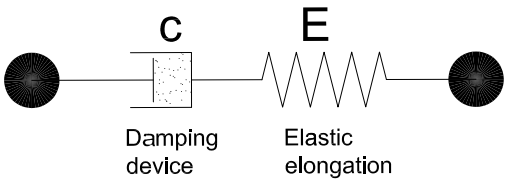

Fig. 10: Viscoelastic Maxwell model.

interphase and therefore should be considered separately. With reference to the viscoelastic Maxwell model, sketched in Fig. 10, it is possible to split the elastic and viscous elongation rates of the outer part of the fibre at the generic time t as follows

$$\dot{u}(t) = \dot{u}_e(t) + \dot{u}_v(t) = \frac{L_e \dot{N}(t)}{EA} + \frac{N(t)}{c}. \tag{12}$$

with " $\cdot$ " indicating the derivative with respect time. The displacements of the section of the fibre where the load is applied at time t is equal to $s = mt$, then by integrating $\dot{u}_v$ from Eq.(12) one obtains

$$u_v(t) = \frac{1}{c}\int_0^t N(\tau)d\tau = \frac{1}{cV}\int_0^s N(s)ds. \tag{13}$$

Now, at the end of the pull-out test it is $N = 0$, thus also the elastic displacement should be $u_e = 0$. In this way the damping coefficient c can be found from the residual viscous displacement according to

$$u_{v,res} = s_{2,f} - L = \frac{1}{cV}\int_0^{s_{2,f}} P(s)ds, \tag{14}$$

being $s_{2,f}$ the displacement of the outer part of the fibre at the end of the test. The integral in Eq.(14) can be computed as the area under the load-displacement curve obtained from the experimental pull-out test. This simple model allows to subtract to experimental data the viscous contribution and to compare them with the elastic analytical model here proposed.

Results and Discussions

Experimental tests

Figure 14 reports the mean experimental curves in terms of axial strain of the outer section of the fibre as a function of adimensional slip at the same cross-section, obtained for several kinds of fibres subjected to pull-out tests. Besides, the theoretical curve obtained form the analytical model is also displayed. The pull-out behaviour of partially recycled synthetic fibres out of the mechanical test is shown in Fig.14(c). For the sake of comparison, results for virgin PP with and without silica coating are also reported in Fig.14(a) and (b), respectively, and experimental data are used for calibrating the constitutive parameters [17]. Analysing the experimental results, the three kinds of fibres here compared exhibit different response against pull-out. Untreated PP fibres (UT-PP) attain the peak strain (namely the imposed axial load N) at the transition between debonding and pull-out stages, whereas S-PP fibres reach the maximum value during the pull-out stage, in compliance with the observations by Di Maida et al. for fibres immersed in basic-catalysed silica bath for long time [15, 21]. In the latter case, the hardening attitude appears even more pronounced due to the particular coating technique. As expected, the initial quasi-linear trend is similar for UT-PP and silica-coated PP (S-PP) fibres,

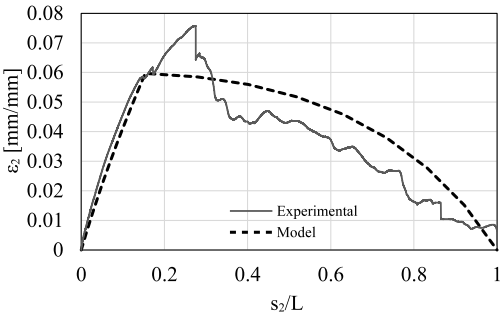

Fig. 11: *
(a) Untreated PP virgin fibres (UT-PP)

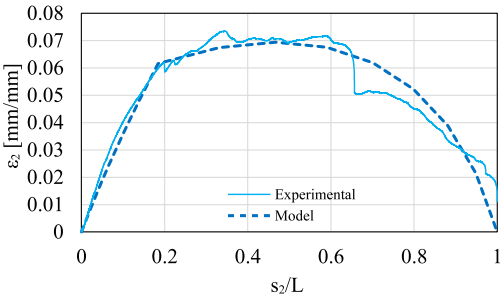

Fig. 12: *
(b) Silica-coated PP virgin fibres (S-PP)

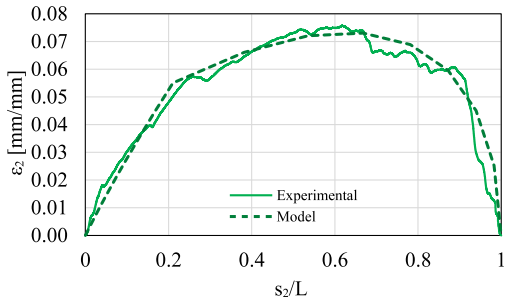

Fig. 13: *
(c) Partially recycled plastic fibres (PRP)

Fig. 14: Variation of axial strain of the outer section of the fibre $\varepsilon_2 = N/EA$ vs s_2/L: comparison between the analytical curves (solid line) and the mean experimental curves (dashed line). Results on PP fibres (a–b) are retrieved from Signorini et al. [17]

whereas partially recycled fibres (PRP) delamination branch develops in a more compliant way, attaining the peak load during the pull-out stage, at a higher slip level, with respect to UT-PP and S-PP fibres. However, the post-peak behaviour significantly differs across the tested groups, especially if PP and recycled fibres are compared. Contrarily to what emerged from UT-PP fibres, both PRP and S-PP fibres attain the maximum load value in the pull-out stage, when friction at the interphase is the leading mechanism. As already pointed out in previous contributions [25, 17, 15], silica coating on synthetic fibres is able to switch the failure mode from friction to tensile rupture of the thin layer of mortar surrounding the fibre, thus resulting in an enhanced overall response.

For what concerns the recycled fibres at hand, the increased friction with mortar can be ascribed to the compresence of unmiscible polymers in the blend, responsible for a rougher surface, as shown in the SEM image in Fig.15, confirming the findings by Signorini and Volpini [13].

Analytical model

Table 1 summarises the constitutive parameters calibrated on the experimental curves shown in the inlets of Fig.14. In this section, the comparison between the experimental and analytical results is discussed. The three parameters τ_0, a, b of the constitutive model are determined by fitting the theoretical curves with the experimental ones concerning recycled PRP fibres, and compared with virgin PP fibres (UT-PP and S-PP) from a couple of diverse datasets. The viscous contribution turns out to be more appreciable for the treated fibres because the pull-out tensile load is higher than for untreated ones. In particular, meanwhile treated fibres require a significant load level till the complete fibre pull-out, the untreated ones display a complete loss of strength, much before the end of the debonding phase. The parameter τ_0 is clearly the one playing the crucial role in the description of the pull-out behaviour of fibres, pointing out the stress threshold for slip to be triggered. Remarkably, PP fibres studied in two different experimental campaigns carried out independently present consistent

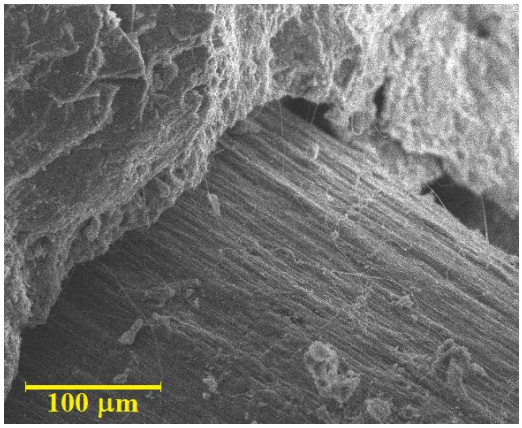

Fig. 15: Abrasion exerted by the matrix on the recycled fibre's surface, responsible for a pronounced increase of shear stress during extraction.

Table 1: Constitutive parameters of the interphase law here proposed and assessment of the accuracy of the model in terms of adimensional dissipated energy

Description	Ref.	Constitutive parameters			Dissipated Energy		
		τ_0 [N mm^{-2}]	a [$\cdot 10^{-2}$N mm^{-3}]	b [$\cdot 10^{-4}$N mm^{-4}]	Exp [$\cdot 10^{-2}$]	Model [$\cdot 10^{-2}$]	Δ [%]
Recycled PE-PET fibres	—	0.670	6.748	0.243	5.449	5.577	2.4
Untreated PP fibres	[17]	0.370	0.723	0.486	3.677	4.111	11.8
Untreated PP fibres	[15]	0.231	2.410	2.430	1.090	0.825	24.3
Silica-coated PP fibres	[17]	0.566	2.900	0.243	5.242	5.228	0.3
Silica-coated PP fibres	[15]	0.300	7.500	20.000	2.193	2.253	2.7

results, ranging from 0.231 to 0.370 N mm^{-2}. The value of τ_0 for recycled fibres turns out to be unexpectedly higher (0.670 N mm^{-2}) as a consequence of the enhanced mechanical grip induced by the rough surface, if compared with the smooth and polished one of PP fibres (see [17, Fig.5a]). Indeed, the value of normalised energy dissipated at complete extraction for PRP and S-PP fibres turns out to be comparable, relying on the experimental evidence by Signorini et al. [17], whereas it appears even higher if compared with S-PP fibres investigated by Di Maida et al. [15]. Anyway, silica coatings lead to beneficial effects on the interphase constitutive law of PP fibres, if compared with uncoated ones. This fact is likely explained by the enhanced adhesion and the subsequent switch of failure mode, from a friction-driven delamination, intrinsically unstable and scattered, to tensile rupture of the mortar in the interphase transition zone (ITZ). A gain in the dissipation capability of approximately 42% is obtained, and a three-fold increase in the parameter a is consistently observed in both the experimental activities under exam. This parameter identifies the slope of the hardening branch of the constitutive law and is intrinsically related to the interphase interactions. In this regard too, recycled fibres present a good hardening response, whose reason is again attributable to friction owing to the rough surface, which leads to results very close to the ones obtained by Di Maida et al. [15] for long-time immersion in silica bath.

The analytical model here presented is able to properly describe the two-branch response of synthetic fibres during extraction from a cement-based matrix. The results in terms of dissipated energy are accurately reproduced, with negligible relative errors. Focusing on PP fibres [15, 17], it is also interesting to note that the model better fits the tests involving silica-coated fibres, endorsing the fact that a more predictable and consistent failure mode is induced by the surface functionalisation. The only exception regards the peak value of tests on uncoated fibres by Signorini et al. [17], whose prediction

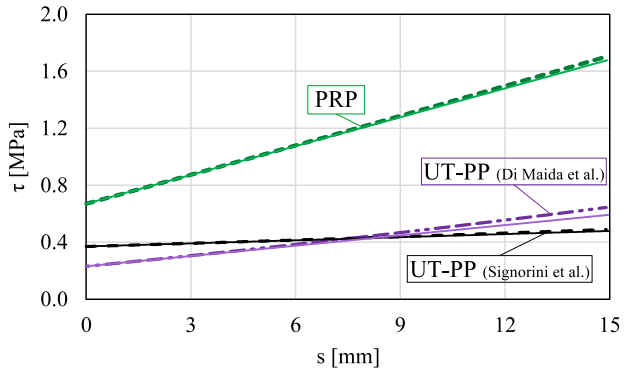

Fig. 16: *

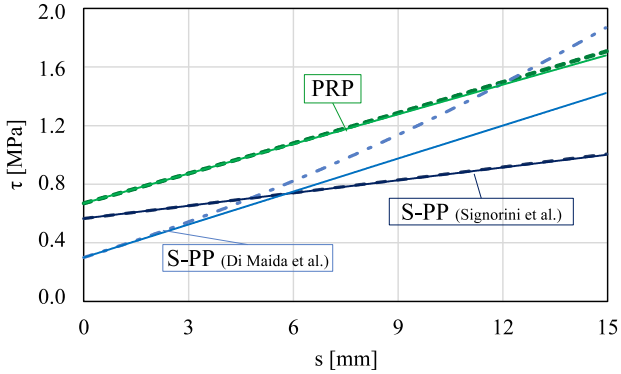

Fig. 17: *

(a) PRP (green) vs. UT-PP fibres (violet – black) (b) PRP (green) vs. S-PP (light-blue – blue)

Fig. 18: Interphase $\tau - s$ constitutive laws for the samples of Table 1. Solid lines identify parabolic slip-hardening laws, whereas dashed and dash-dotted lines refer to linear approximations neglecting the parameter b

is underestimated. Furthermore, the extremely low values of the coefficient b across all the sample groups suggest that the model could be further simplified considering a linear slip-hardening stage in the constitutive law at the interphase, involving only the parameters τ_0 and a. The quasi-linear behaviour is also shown in Figure 18, which juxtaposes the interphase constitutive laws for the 5 groups of samples here discussed and their linear approximation. Only Di Maida et al. datasets about S-PP fibres exhibit a pronounced non-linear behaviour [15]. Sorzia et al. show that constitutive parameters are substantially related to the bonding properties between the fibre and the matrix and regardless of the embedded length of the fibre [21]. Besides, setting correctly τ_0, a, b, the model is able to describe the pull-out test also for different kind of fibres, e.g. steel fibres, with different constitutive behaviours. Furthermore, the comparison carried out on different values of tensile loads and different embedded lengths allows to state that the model is nearly independent on the geometry and loading conditions.

Finally, it is possible to compare the model with the one developed by Radi et al., carried out making reference to the deformed configuration of the fibre and accounting for an initial linear-elastic stage in the frictional bond relationship [22]. The comparison does not highlight considerable differences, meaning that this simple model can achieve the same accuracy on pull-out tests with limited duration, in which the viscous elongation is contained. Wang et al. conjectured a similar frictional bond relationship neglecting the initial linear elastic response of the fibre, because its influence in the whole pull-out process is unimportant [23]. Therefore, this model represents a simplified version of the method proposed by Radi et al. albeit preserving its main features, but taking advantage of a simpler numerical implementation and an easier scheme for the calibration of the constitutive parameters.

Conclusions

The present paper assesses the pull-out response of a partially recycled fibre made of a blend of virgin polypropylene (PP, 30%) and recycled plastic deriving from processing of food packaging industrial waste (polyethylene terephthalate and polyethylene, 70%). A simple analytical model is proposed to study the pull-out behaviour of synthetic fibres considering other 2 experimental activities. This approach could be used to extend the analysis to a more complex model accounting for fibres orientation and distribution. Since the pull-out process is deeply related to the fibre stress bridging during the FRC fracture, the model could allow to evaluate the equivalent flexural strength ratio $R_{e,3}$ and the post-cracking strengths f_{Rj}, which are fundamental for the design of FRC structural elements such beams, slabs and floors [9]. The one-dimensional analytical model presented in this paper is suitable to describe the behaviour of a pull-out test of synthetic fibres embedded in a cement matrix. In spite of

its simplicity, it can also take into account different slip-bonding relationships between the fibre and the surrounding matrix by setting adequately the constitutive parameters. Thus, it can be employed for both different surface treatments and different kinds of fibres. Furthermore, it can be used as a first early study to investigate the toughness and the breakage of FRC structural elements.

Acknowledgements

Financial support from "Progetto IMPReSA" Impiego di Materiali Plastici da Riciclo per malte e calcestruzzi Strutturali Alleggeriti" (POR-FESR 2014/2020 - asse 1.2.2, CUP E81F18000310009) is worth to be mentioned. CS also gratefully acknowledges support from "Progetto Giovani 2020" by the National Group of Mathematical Physics (GNFM-INdAM).

References

[1] A. Remennikov, S. Kaewunruen, Impact resistance of reinforced concrete columns: experimental studies and design considerations.

[2] D.-Y. Yoo, N. Banthia, Impact resistance of fiber-reinforced concrete–a review, Cement and Concrete Composites 104 (2019) 103389.

[3] J. Thomas, A. Ramaswamy, Mechanical properties of steel fiber-reinforced concrete, Journal of materials in civil engineering 19 (5) (2007) 385–392.

[4] D.-Y. Yoo, Y.-S. Yoon, Influence of steel fibers and fiber-reinforced polymers on the impact resistance of one-way concrete slabs, Journal of Composite Materials 48 (6) (2014) 695–706.

[5] D.-Y. Yoo, U. Gohil, T. Gries, Y.-S. Yoon, Comparative low-velocity impact response of textile-reinforced concrete and steel-fiber-reinforced concrete beams, Journal of Composite Materials 50 (17) (2016) 2421–2431.

[6] V. Mechtcherine, O. Millon, M. Butler, K. Thoma, Mechanical behaviour of strain hardening cement-based composites under impact loading, Cement and Concrete Composites 33 (1) (2011) 1–11.

[7] I. Curosu, V. Mechtcherine, D. Forni, E. Cadoni, Performance of various strain-hardening cement-based composites (shcc) subject to uniaxial impact tensile loading, Cement and Concrete Research 102 (2017) 16–28.

[8] L. Lanzoni, A. Nobili, A. M. Tarantino, Performance evaluation of a polypropylene-based draw-wired fibre for concrete structures, Construction and Building Materials 28 (1) (2012) 798–806.

[9] E. Radi, P. Di Maida, Analytical solution for ductile and frc plates on elastic ground loaded on a small circular area, Journal of Mechanics of Materials and Structures 9 (3) (2014) 313–331.

[10] L. Lanzoni, A. Nobili, E. Radi, A. Sorzia, Failure mechanism of FRC slabs on non-local ground, Meccanica 51 (10) (2016) 2473–2492.

[11] L.-f. Liu, P.-m. Wang, X.-j. Yang, Effects of characteristics of polypropylene fiber on anti-dry-shrinkage cracking property of cement mortar, Journal of Building Materials 3.

[12] F. Fraternali, V. Ciancia, R. Chechile, G. Rizzano, L. Feo, L. Incarnato, Experimental study of the thermo-mechanical properties of recycled pet fiber-reinforced concrete, Composite Structures 93 (9) (2011) 2368–2374.

[13] C. Signorini, V. Volpini, Mechanical performance of fiber reinforced cement composites including fully-recycled plastic fibers, Fibers 9 (3) (2021) 16.

[14] X. Dong, Y. Ding, T. Wang, Spalling and mechanical properties of fiber reinforced high-performance concrete subjected to fire, Journal of Wuhan University of Technology-Mater. Sci. Ed. 23 (5) (2008) 743–749.

[15] P. Di Maida, E. Radi, C. Sciancalepore, F. Bondioli, Pullout behavior of polypropylene macro-synthetic fibers treated with nano-silica, Construction and Building Materials 82 (2015) 39–44.

[16] P. Di Maida, C. Sciancalepore, E. Radi, F. Bondioli, Effects of nano-silica treatment on the flexural post cracking behaviour of polypropylene macro-synthetic fibre reinforced concrete, Mechanics Research Communications 88 (2018) 12–18.

[17] C. Signorini, A. Sola, B. Malchiodi, A. Nobili, A. Gatto, Failure mechanism of silica coated polypropylene fibres for fibre reinforced concrete (FRC), Construction and Building Materials 236 (2020) 117549.

[18] B. Felekoglu, K. Tosun, B. Baradan, A comparative study on the flexural performance of plasma treated polypropylene fiber reinforced cementitious composites, Journal of Materials Processing Technology 209 (11) (2009) 5133–5144.

[19] C. Signorini, A. Sola, B. Malchiodi, A. Nobili, Highly dissipative fiber-reinforced concrete for structural screeds, Journal of Materials in Civil Engineering under review.

[20] F. Deng, X. Ding, Y. Chi, L. Xu, L. Wang, The pull-out behavior of straight and hooked-end steel fiber from hybrid fiber reinforced cementitious composite: Experimental study and analytical modelling, Composite Structures 206 (2018) 693–712.

[21] A. Sorzia, L. Lanzoni, E. Radi, Pullout modelling of viscoelastic synthetic fibres for cementitious composites, Composite Structures 223 (2019) 110898.

[22] E. Radi, L. Lanzoni, A. Sorzia, Analytical modelling of the pullout behavior of synthetic fibres treated with nano-silica, Procedia Engineering 109 (2015) 525–532.

[23] Y. Wang, V. C. Li, S. Backer, Modelling of fibre pull-out from a cement matrix, International Journal of Cement Composites and Lightweight Concrete 10 (3) (1988) 143–149.

[24] Z. Lin, V. C. Li, Crack bridging in fiber reinforced cementitious composites with slip-hardening interfaces, Journal of the Mechanics and Physics of Solids 45 (5) (1997) 763–787.

[25] Z. Cohen, A. Peled, Effect of nanofillers and production methods to control the interfacial characteristics of glass bundles in textile fabric cement-based composites, Composites Part A: Applied Science and Manufacturing 43 (6) (2012) 962–972.